

# RSC Advances



This is an *Accepted Manuscript*, which has been through the Royal Society of Chemistry peer review process and has been accepted for publication.

*Accepted Manuscripts* are published online shortly after acceptance, before technical editing, formatting and proof reading. Using this free service, authors can make their results available to the community, in citable form, before we publish the edited article. This *Accepted Manuscript* will be replaced by the edited, formatted and paginated article as soon as this is available.

You can find more information about *Accepted Manuscripts* in the [Information for Authors](#).

Please note that technical editing may introduce minor changes to the text and/or graphics, which may alter content. The journal's standard [Terms & Conditions](#) and the [Ethical guidelines](#) still apply. In no event shall the Royal Society of Chemistry be held responsible for any errors or omissions in this *Accepted Manuscript* or any consequences arising from the use of any information it contains.



## Investigations on rate performance of polyol technique developed LiFePO<sub>4</sub>/CeO<sub>2</sub> composite materials for Rechargeable Lithium batteries

Received 00th January 20xx,  
Accepted 00th January 20xx

DOI: 10.1039/x0xx00000x

www.rsc.org/

M. Sivakumar\*, R. Muruganatham and R. Subadevi

An attempt has been made to synthesize the CeO<sub>2</sub> modified LiFePO<sub>4</sub> composite cathode materials via polyol technique with chemical combination route. The surface modified LiFePO<sub>4</sub> samples exhibits superior electrochemical performances than bare. CeO<sub>2</sub> may aid to induce the fast lithium-ion diffusivity of LiFePO<sub>4</sub> cathode materials to promote the high-rate, stable cyclic and good coulombic efficiency. The complete coverage of mild coating of CeO<sub>2</sub> under optimized concentration on LiFePO<sub>4</sub> may limit the direct contact of the active material with the electrolyte, which improves the interface stability by preventing dissolution of Fe-ions in the electrolyte.

### 1. Introduction

Olivine-structured LiFePO<sub>4</sub> (LFP) has been highlighted as one of the most promising cathode materials for rechargeable lithium-ion batteries (LIBs) because of its environmental compatibility, low cost, high capacity and thermal stability. [1, 2] However, the inherent low ionic and electronic conductivities of LiFePO<sub>4</sub> significantly detain the electrochemical performance; especially at high-rate. The surface coating technology plays an important role in the electrochemical performance of cathode materials. Surface coating has been divided into three different configurations such as rough coating [3], core shell structure coating [4, 5] and ultra thin film coating. [6] Surface coating has been proven to be effective for improving the capacity retention, rate capability and even thermal stability of cathode materials for lithium ion batteries. [7, 8] In recent years, the surface coating/modification of LiFePO<sub>4</sub> with different materials such as carbon [9, 10], metal oxides [11-13], fluorides [14] and metal phosphates [15], etc has been investigated. However, metal or non metal oxide significantly improved the electrochemical performance and most of the oxides are reported as electrochemical inactive oxides or semiconductor oxides, where as electronic conductivity is lower.

Cerium (IV) oxide and CeO<sub>2</sub>-containing materials are intensively studied as catalysts in numerous three-way catalyst formulations. Yao et al. [16] and Liu et al. [7] reported that the electrochemical properties of pristine LiFePO<sub>4</sub> electrode were improved when LiFePO<sub>4</sub> electrodes were modified with CeO<sub>2</sub>. They suggested that modification with CeO<sub>2</sub> is an effective way

to improve the electrochemical properties of LiFePO<sub>4</sub> cathode material. CeO<sub>2</sub> modification could enhance the ionic conductivity of LiFePO<sub>4</sub> and produce a good electrical contact between oxides. Also, the resistance between the electrolyte and electrode has been reduced. [17-19] Quan et al. [20] introduced the effects of CePO<sub>4</sub> tailored LiFePO<sub>4</sub> in the form of LiFePO<sub>4</sub>/C/CePO<sub>4</sub> composites. CeO<sub>2</sub> is a good oxygen storage material based on the reversible redox reaction. However, the LFP modification using CeO<sub>2</sub> via polyol technique has been rarely carried out in the literature. Therefore, an attempt has been made to prepare the cerium metal oxide (CeO<sub>2</sub>) tailored LiFePO<sub>4</sub> via suitable economic energy-efficient polyol technique. The structural, morphological, chemical and electrochemical performance of the prepared materials were systematically studied in detail.

### 2. Experimental

#### 2.1. Synthesis of cerium oxide coated LiFePO<sub>4</sub>

LiFePO<sub>4</sub> cathode material was prepared via conventional polyol technique. [11, 21, 22] The starting materials, iron (II) sulphate heptahydrate (FeSO<sub>4</sub>·7H<sub>2</sub>O, 99.9 % of Alfa-Aesar) and lithium dihydrogen phosphate (LiH<sub>2</sub>PO<sub>4</sub>, 99.9 % of Alfa-Aesar) were taken in stoichiometric molar ratio and dissolved in diethylene glycol (DEG, Aldrich), a polyol solvent. The mixed solution was heated closer to the boiling point of the polyol solvent (245 °C) for 18 h under a refluxing process. After that, the reacted solution was washed several times with ethanol and acetone. The resulting particles were separated and dried in a vacuum oven at 150 °C for 48 h; to obtain the uncoated-LiFePO<sub>4</sub> (bare LFP) sample. 1, 2 and 3 wt. % of Ce (NO<sub>3</sub>)<sub>3</sub>·6H<sub>2</sub>O and 0.3 N NH<sub>4</sub>OH were dissolved in distilled water, in which the prepared LiFePO<sub>4</sub> was dispersed at room temperature. The mixture was slightly heated and maintained at a temperature

# 120, Energy Materials Lab, School of Physics, Alagappa University, Karaikudi-630 004, Tamil Nadu, India. E-mail: susiva73@yahoo.co.in (M.Sivakumar)

of 50 °C while being stirred in order to evaporate the solvent. The resulting particles were heated at 500 °C for 1 h under Argon atmosphere. Finally, CeO<sub>2</sub>-coated LiFePO<sub>4</sub> composite materials were obtained.

## 2.2. Structure, morphological and elemental characterizations

The powder X-ray diffraction (XRD) analyses of uncoated and coated LiFePO<sub>4</sub> samples were performed using a PANalytical X-pert diffractometer with a CuK<sub>α</sub> radiation operated at 40 kV, 30 mA and the wavelength of  $\lambda = 1.54060 \text{ \AA}$  in the range  $2\theta = 10\text{--}70^\circ$ . The functional group vibration was analysed using Thermo Nicolet 380 FT-IR spectrophotometer using KBr pellets in the range 4000–400 cm<sup>-1</sup>. The morphology of prepared materials were studied by using field emission scanning electron microscopy (FESEM, LEO-1530, ZEISS, Germany), energy dispersive spectrometer (EDS, X-MAX50, 30 kV). The nano particles and coating of CeO<sub>2</sub> were observed by high resolution transmission electron microscopic (HR-TEM) (Techni G2 S-TWIN, FEI, Netherlands) techniques. Chemical valence states of the elements were investigated by X-ray photoelectron spectroscopy (XPS, PHI model 5802).

## 2.3. Fabrication of coin cell and electrochemical studies

A Li-metal |LiPF<sub>6</sub> (EC+DMC)| CeO<sub>2</sub> coated LiFePO<sub>4</sub> cell was used to investigate the electrochemical performances of the prepared composite cathodes using CR2032 type coin cells. The cathodes (positive electrode) were prepared by mixing of 80 wt. % CeO<sub>2</sub>/LiFePO<sub>4</sub> composite powder, 10 wt. % super P, and 10 wt. % Poly-(vinylidene fluoride) (PVdF) in N-methylpyrrolidone (NMP) solvent to form a homogeneous slurry. Then, the mixed slurry was spread uniformly on a thin aluminum foil and dried in vacuum at 120 °C for 6 h and then roll pressed; then the samples were punched into circular discs. Polypropylene separator (Celgard 2400, Hoechst Celanese Corp) was drenched in the electrolyte for 24 h prior to use. The coin cell assembling procedures were performed using Ar-filled glove box by keeping both the oxygen and moisture levels less than 1 ppm. The galvanostatic charge-discharge analysis was performed using a BTS-55 Neware battery testing system between the potential 2.5 and 4.5 V (vs. Li/Li<sup>+</sup>) at ambient temperature with different C-rates. Electrochemical impedance (EIS) analysis was performed on a CHI 660D electrochemical analyser (CH Instruments) at room temperature in the frequency range 10<sup>6</sup>–0.01 Hz with AC signal amplitude of 5 mV.

## 3. Results and discussion

### 3.1. Structural studies

Figure 1 shows the XRD patterns of bare and CeO<sub>2</sub>-coated LiFePO<sub>4</sub> cathode materials with the standard data. The pristine and CeO<sub>2</sub>-coated LiFePO<sub>4</sub> materials have been confirmed to possess a well-defined orthorhombic olivine structure with a space group of Pnma (JCPDS 83-2092). The diffraction peaks of CeO<sub>2</sub> are not appearing in 1 wt. % based sample is due to low content of CeO<sub>2</sub> in the precursor. [23] Figure 1 (c, d) shows the existence of two minor peaks appeared at  $2\theta = 29$  and  $33^\circ$  of (1 1 1) and (2 0 0) planes corresponding to 2 and 3 wt. % of CeO<sub>2</sub> coated LiFePO<sub>4</sub> sample, respectively. The presence of impurity

peaks suggests that the CeO<sub>2</sub> has formed a thin solid solution layer on the surface of LiFePO<sub>4</sub> particles. CeO<sub>2</sub> has been confirmed by standard crystal diffraction data and literature reports (JCPDS 89-8436). [24, 25] Hence, the CeO<sub>2</sub> coating does not change the structure of bare LiFePO<sub>4</sub>. These results indicate that cerium oxide is just coated on the surface of LiFePO<sub>4</sub> particles. The poor crystallinity of CeO<sub>2</sub> is due to the precursor has been calcined at low temperature with short duration (500° for 1h), which results in the disappearance of the face-centered cubic CeO<sub>2</sub> peaks in the CeO<sub>2</sub> coated samples. Similar phenomenon can be observed in the earlier reports of rare earth oxide modified sample after calcination at the low temperature (400 °C). [16, 26, 27]

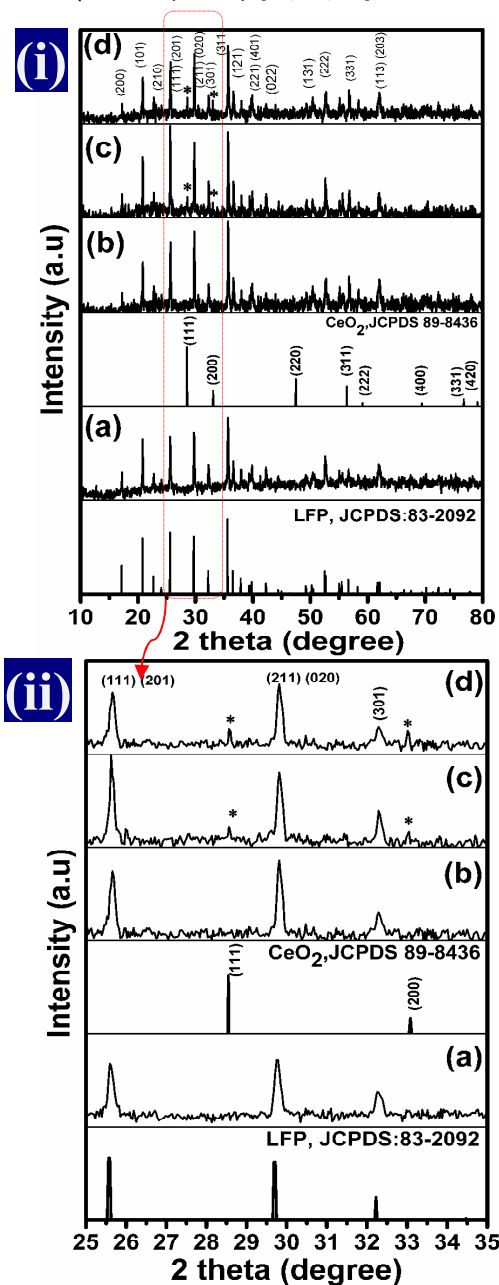


Fig. 1 XRD patterns of (i) (a) bare LiFePO<sub>4</sub>, (b-d) 1 to 3 wt. % of CeO<sub>2</sub> coated LiFePO<sub>4</sub> and (ii) enlarged patterns of selected  $2\theta$  range.

The crystallite size ( $D$ ) has been calculated using Scherrer's equation  $D = K\lambda/b \cos\theta$ , where  $D$  is the crystallite size,  $K$  is the shape factor (0.9), and  $\lambda$  wavelength of X-ray,  $b$  is the full width at half maximum (FWHM) and  $\theta$  is the Bragg's angle. The calculated crystal lattice parameters and average crystallite sizes for all samples are shown in Table 1.

Table 1. The lattice parameters and crystallite sizes of uncoated and coated samples from XRD data

Samples name	JCPDS No. 83-2092	LiFePO <sub>4</sub>	1 wt % coated LiFePO <sub>4</sub>	2 wt % coated LiFePO <sub>4</sub>	3 wt % coated LiFePO <sub>4</sub>
<b>Structural parameters</b>					
<b>Lattice constant values and volume</b>	a= 10.33 Å b= 6.010 Å c= 4.693 Å V=291.4 Å <sup>3</sup>	a= 10.3142 Å b= 6.0022 Å c= 4.6842 Å V= 292.08 Å <sup>3</sup>	a= 10.3141 Å b= 6.0020 Å c= 4.6842 Å V= 291.81 Å <sup>3</sup>	a= 10.3139 Å b= 6.0019 Å c= 4.6843 Å V= 292.08 Å <sup>3</sup>	a= 10.3137 Å b= 6.0018 Å c= 4.6843 Å V= 291.81 Å <sup>3</sup>
<b>Average Crystallite sizes (nm)</b>	--	51	52	53	59

The slight change in cell parameter values indicates that the presence of CeO<sub>2</sub> on LiFePO<sub>4</sub> surface and doesn't affect the structure of bare LiFePO<sub>4</sub>. It indicates that CeO<sub>2</sub> did not diffuse into LiFePO<sub>4</sub> lattice; it is mere coat on the surface of LiFePO<sub>4</sub> and could form the solid solution. Also, the average crystallite sizes are slightly increased with the increase of coating content and do not change the phase structure of LiFePO<sub>4</sub>, similarly as other coating materials. [26, 27] However, due to the coating procedure was carried out at 500 °C, few amorphous particles may have been attached on the surface of the core material.

Figure 2 (a-d) shows the FT-IR spectra of the bare and CeO<sub>2</sub> coated LiFePO<sub>4</sub> samples. The band between 932 and 1134 cm<sup>-1</sup>, corresponds to the symmetric and antisymmetric stretching mode of P-O vibration peak of PO<sub>4</sub> tetrahedron in defect-free LiFePO<sub>4</sub>. Symmetric and antisymmetric O-P-O bending modes exist in the range of 460-633 cm<sup>-1</sup>. [28] The bending and stretching modes of bare and coated samples have been observed in the range 460-1134 cm<sup>-1</sup>. In addition, no additional peaks are observed in the bare LiFePO<sub>4</sub> material.

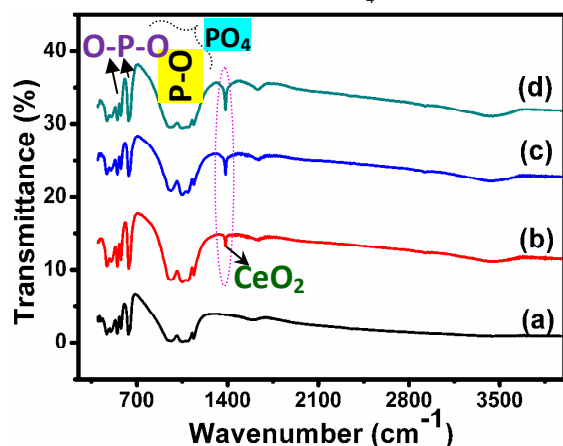


Fig. 2 (a-d) FT-IR spectra of bare, 1, 2 and 3 wt. % CeO<sub>2</sub> coated LiFePO<sub>4</sub> samples.

The presence of CeO<sub>2</sub> in the coated LiFePO<sub>4</sub> is confirmed through the band at 1381 cm<sup>-1</sup>, which is the characteristic vibration mode of CeO<sub>2</sub> stretching vibration. [29, 30]

The intensity of the vibrational peaks increases with the increase of CeO<sub>2</sub> content. The O-H bending and stretching vibrations are located at 1628 and 3436 cm<sup>-1</sup>. It may be due to the lower calcination temperature or absorbed water molecule from air during the analysis, since, Ceria is slightly hygroscopic in nature.

### 3.2. Morphological and Elemental analysis

The SEM images of the bare, 1, 2 and 3 wt. % of CeO<sub>2</sub>-coated LiFePO<sub>4</sub> materials are shown in Figure 3 (a-d). The bare LiFePO<sub>4</sub> material has long rod-like particles with the average size 350 nm × 100 nm of length × width. The calcination results in breaking the lengthy rods into smaller rods and few grains on its surface. It exhibits the agglomeration between the grains, which are found lesser in coated samples than the bare one. The average particle sizes were measured as length × breadth (250 × 80), (128 × 56) and (180 × 65) nm respectively for the 1, 2 and 3 wt. % of CeO<sub>2</sub> coated LiFePO<sub>4</sub> samples by 'measureIT' software (Olympus soft imaging solution GMBH product). As the content of CeO<sub>2</sub> is increased, the solid solution or nano-sized CeO<sub>2</sub> particles growth is increased on LFP surface. The surface modification on LiFePO<sub>4</sub> would affect the electrochemical properties.

The energy dispersive X-ray (EDX) analysis was carried out to identify the elemental atoms presence. Figure 4 (a-d) illustrates that the EDX spectra of bare, 1, 2 and 3 wt. % CeO<sub>2</sub> coated LFP samples. According to EDX results, a new phase containing Ce was detected in coated samples. These results are in good agreement with the actual CeO<sub>2</sub> content used in the coated LFP materials. Also, from this analysis, we can calculate the ratio of the elemental atoms such as Fe/P is almost equal to 1 and O/Fe or O/P is equal to 4, which gives an additional confirmation of LiFePO<sub>4</sub> formation.

Figure 5(a-c) clearly shows the TEM images of 1, 2 and 3 wt. % of CeO<sub>2</sub> coated LFP particles. It is apparent from the TEM images (Figure 5(a-c)) that there are two distinct morphologies; dark part representing LiFePO<sub>4</sub> and lighter part representing CeO<sub>2</sub> particles or solid solution layer. Figure 5b demonstrates that 2 wt. % of CeO<sub>2</sub> has been coated as thin layer on the surface of LiFePO<sub>4</sub> particles. Figure 5c reveals the existence of few particles and layers on the surface of core particles. The related SAED pattern (Fig. 5(d-f)) exhibits a regular and clear diffraction spot array, which indicates that the particle is single-crystalline and it can be indexed to orthorhombic phase of LiFePO<sub>4</sub>. These results are in good agreement with the XRD results.

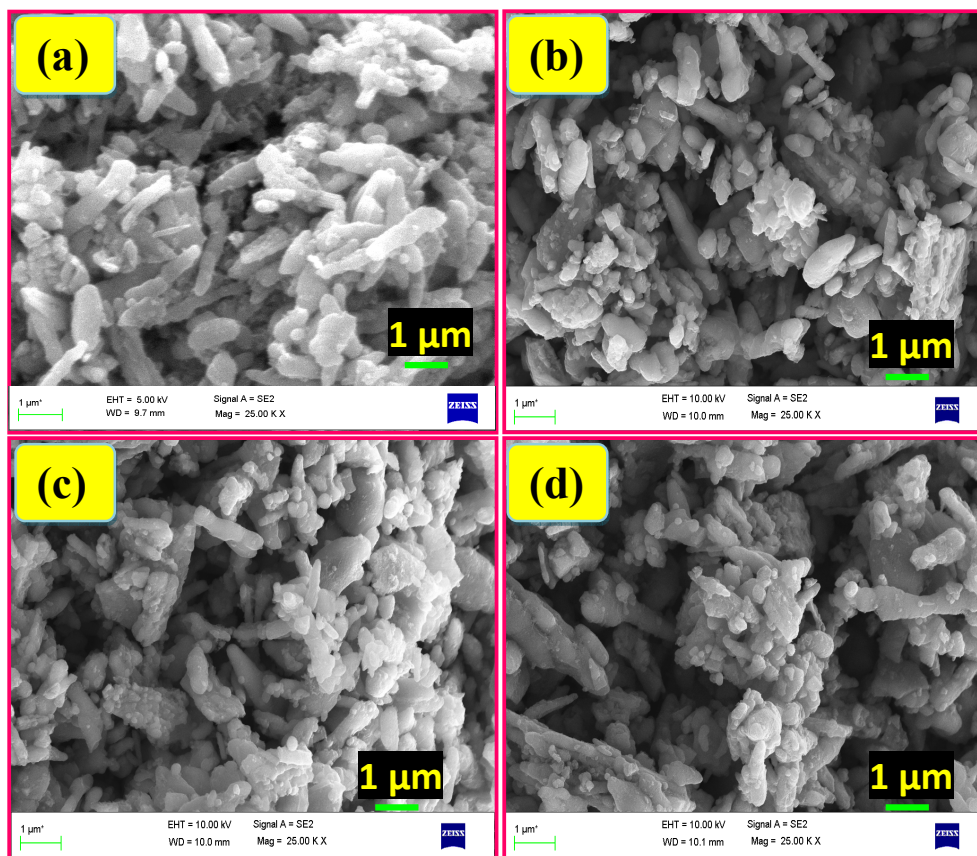


Fig. 3 (a-d) SEM images of bare, 1, 2 and 3 wt. % CeO<sub>2</sub> coated LiFePO<sub>4</sub> samples.

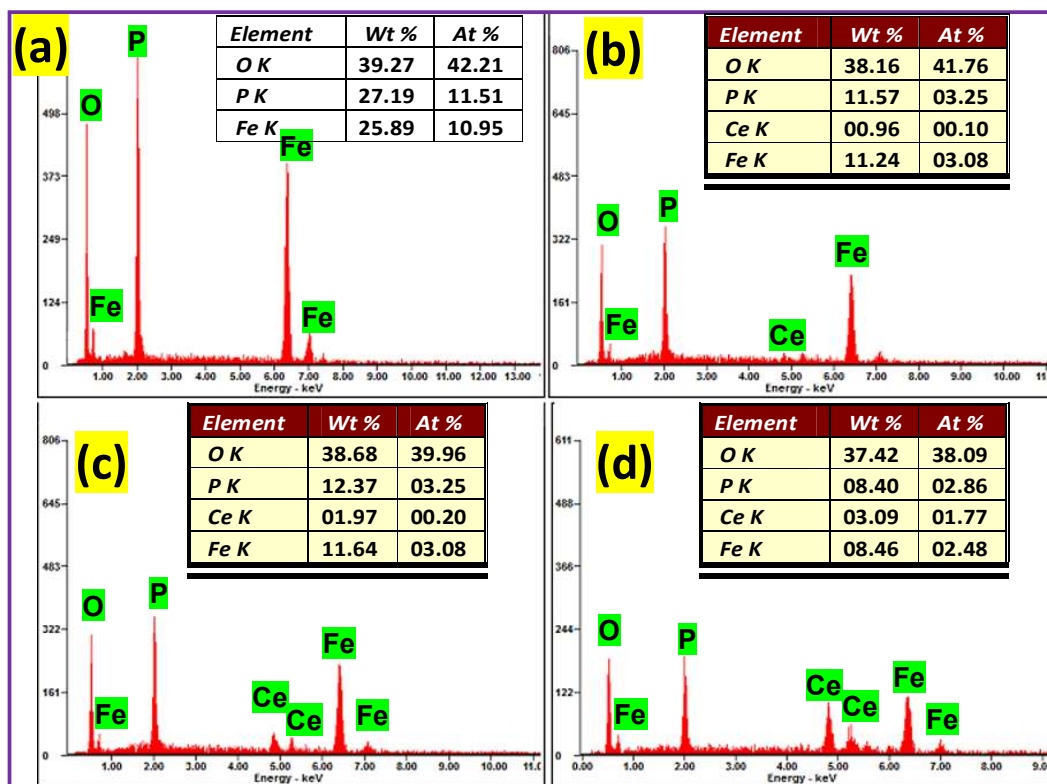
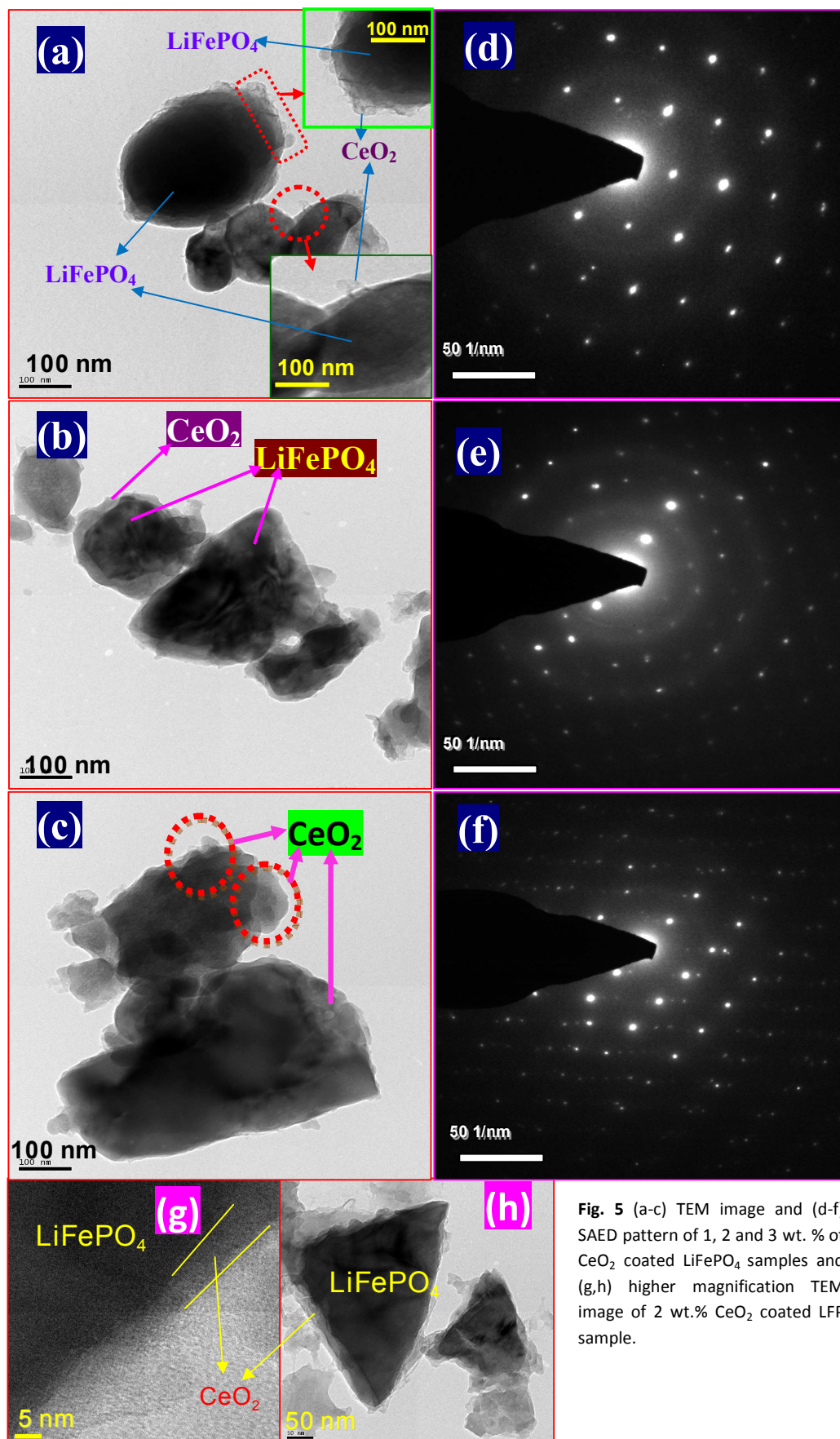


Fig. 4 (a-d) EDX spectra of bare, 1, 2 and 3 wt. % CeO<sub>2</sub> coated LiFePO<sub>4</sub> samples.



**Fig. 5** (a-c) TEM image and (d-f) SAED pattern of 1, 2 and 3 wt. % of CeO<sub>2</sub> coated LiFePO<sub>4</sub> samples and (g,h) higher magnification TEM image of 2 wt.% CeO<sub>2</sub> coated LFP sample.

The surface composition and the oxidation state of the elements were analysed by X-ray photoelectron spectroscopy (XPS). Figure 6a shows the wide range core spectra of 2 wt. % CeO<sub>2</sub> coated LiFePO<sub>4</sub> composite and the results confirm the presence of all elements in the prepared sample. Figure 6 (b-f) demonstrates the core spectra of Li 1s, Fe 2p, P 2p, O 1s and Ce 3d respectively. Figure 6c (Fe 2p) has been splitted into two components, because of spin-orbit coupling, namely Fe 2p<sub>3/2</sub> and Fe 2p<sub>1/2</sub>. LiFePO<sub>4</sub> shows Fe 2p<sub>3/2</sub> main peaks at 710 eV and 724 eV for Fe 2p<sub>1/2</sub>, which are in good agreement with Fe<sup>2+</sup> in LiFePO<sub>4</sub>. [31]

The presence of carbon (C1s) peak is denoted that the minor contribution of oxygenated carbon at the surface of prepared material. The O 1s binding energy (B.E) has been observed at 530.46 eV is corresponding to the lattice oxygen (O<sup>2-</sup>) of the orthorhombic structure. [32, 33] The XPS spectrum of Ce is complex and splitted into Ce3d<sub>3/2</sub> and Ce3d<sub>5/2</sub> with multiple shake-up and shake-down satellites. The peaks between 875 and 895 eV belong to the Ce3d<sub>5/2</sub>, while peaks between 895 and 910 eV correspond to the Ce3d<sub>3/2</sub> levels. [34, 25] The peak at 916 eV is a characteristic satellite peak indicates the presence of CeO<sub>2</sub> (IV). [35] Thus, the XPS analysis confirms the presence of elements in the as-prepared material.

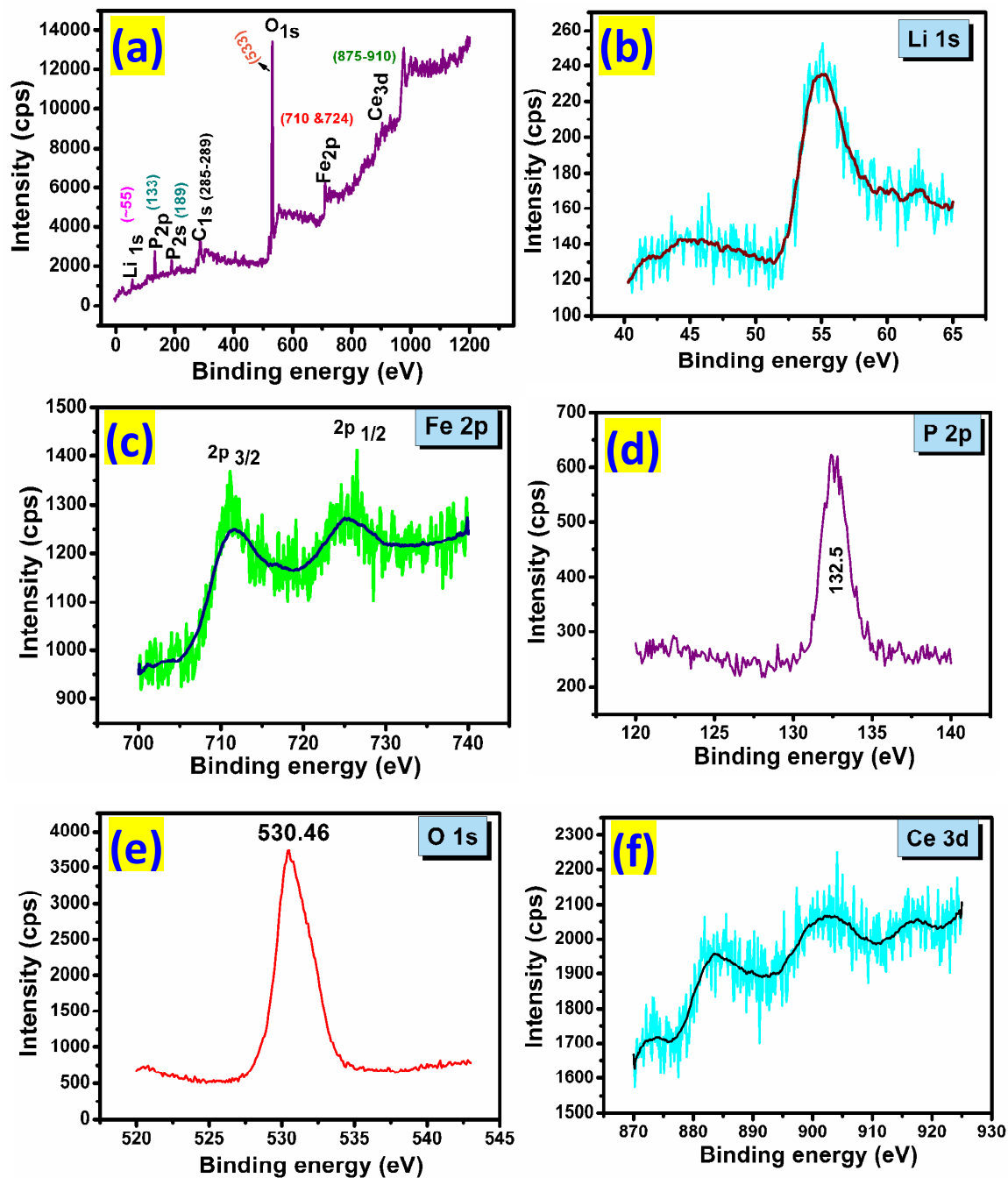


Fig. 6 X-ray photoelectron spectra of 2 wt. % CeO<sub>2</sub> coated LiFePO<sub>4</sub> composite (a) wide range (b) Li 1s (c) Fe (d) P (e) O and (f) Cerium.

### 3.3. Electrochemical studies

The electronic conductivity of the cathode material is very important for lithium intercalation/de-intercalation processes in the lithium ion cell. The electronic conductivities of the pristine and CeO<sub>2</sub> coated LFP samples are shown in Table 2. The electrical conductivity of the synthesized materials was determined by using a four-probe DC method. It is shown that the electronic conductivities of coated samples are increased, when compared to pristine LFP. [36] Electrical conductivity is a physical property reflecting the ability of a matter to transfer electrical charge. The ionic mobility is depending on many factors, but mostly the size of ions and ionic bond strength. Therefore, an enhancement of conductivity is used to induce the EC performance of LFP electrode material. The electronic conductivity of the active material has played a vital role in the transfer of charge from the current collector during the charging and discharging process. The actual lithium ionic conduction has been taken place between the electrodes through the electrolyte in the Li/electrolyte/LiFePO<sub>4</sub> coated using CeO<sub>2</sub> cell couple. Normally, for bare LiFePO<sub>4</sub>, the electronic conductivity is very low. Therefore, the charge transfer from the electrode material to the current collector was not upto the mark. But, after coating the CeO<sub>2</sub> on LiFePO<sub>4</sub> in an optimum level, the transferring of charge is excellent and exhibits appreciable performances than the bare material. [37]

Table 2 Electronic conductivities of the pristine and CeO<sub>2</sub> coated LiFePO<sub>4</sub> samples under room temperature.

Sample name	Electronic conductivity
Bare LiFePO <sub>4</sub>	$2.88 \times 10^{-2} \text{ S cm}^{-1}$
1wt.%CeO <sub>2</sub> -LiFePO <sub>4</sub>	$5.01 \times 10^{-2} \text{ S cm}^{-1}$
2wt.% CeO <sub>2</sub> -LiFePO <sub>4</sub>	$7.03 \times 10^{-2} \text{ S cm}^{-1}$
3wt.% CeO <sub>2</sub> -LiFePO <sub>4</sub>	$6.25 \times 10^{-2} \text{ S cm}^{-1}$

Figure 7a shows the initial charge/discharge curves of the pristine, 1, 2 and 3 wt. % CeO<sub>2</sub>-coated LiFePO<sub>4</sub> samples at 0.1 C rate under room temperature. All the cells exhibited discharge voltage plateaus around 3.45 V, which is the main characteristic of the two-phase reaction of the Lithium extraction and insertion between LiFePO<sub>4</sub> and FePO<sub>4</sub>. [29] The initial charge/discharge capacity of pristine LiFePO<sub>4</sub> is 152/149 mAhg<sup>-1</sup>, whereas for 1, 2 and 3 wt. % CeO<sub>2</sub>-coated LiFePO<sub>4</sub>, it is 157/153, 164/163 and 160/159 mAhg<sup>-1</sup> at 0.1 C rate, respectively. This value of coated LFP is higher when compared to the bare sample, which is due to the electronic conductivity has been improved after the surface treatment. Obviously, the metal oxide coated cathode particles surface may limit the direct contact of the active material with the electrolyte, i.e., the metal oxide particles cover the core material. This improves interface stability and prevents the dissolution of Fe-ions in the electrolyte. [38]

Figure 7b demonstrates the charge/discharge profile at 1 C rate under room temperature for all coated LFP samples up to 50 cycles. Among samples studied, the 2 wt. % of CeO<sub>2</sub> coated on LiFePO<sub>4</sub> shows better discharge capacity with cyclic stability and retention when compared with 1 and 3 wt. % of CeO<sub>2</sub> coated LiFePO<sub>4</sub> composites. There are several factors affect the electrochemical performances of the prepared materials:

(i) the capacity increases upon increasing CeO<sub>2</sub> content until 2 wt. %, which is due to the improvement of electronic conductivity of the material. The coverage of solid solution layer on its surface, which provides a better electrode-electrolyte contact and reduce the polarization of bare material (inset Figure 7a); it causes an enhancement in electronic conductivity, (ii) 2 wt. % of CeO<sub>2</sub> coated LFP sample exhibits better capacity, retention and cyclic capability among the other samples studied. This is due to complete coverage of thin layer of CeO<sub>2</sub> solid solution, which may enhance the structural stability and improve the ionic/electronic conductivity of the bare LFP material [24, 26], (iii) Further increment of CeO<sub>2</sub> causes the aggregation of the cerium oxide particles and thick layer on the surface of LiFePO<sub>4</sub>, which leads to the crystallite regions, and the CeO<sub>2</sub> particles tend to impede ionic movement by acting as mere insulators. An optimal content of CeO<sub>2</sub> addition would result in enhancing the electrochemical properties [24]; whereas beyond the optimal content of CeO<sub>2</sub>, the electrochemical performance rescinds since its higher content lead to an inactive or insulating nature. Similar observation has already been made by Ha et al. [39] and Liu et al. [7]

Recently, most of the high rate applications like (electric vehicles) EV, (heavy electric vehicles) HEV, (high energy density) HED batteries, etc. are occupied the current commercial market due to the appealing rate performance and cycling capability. [38] In the present study the high rate studies for the cells have been performed and have given in Figure 7c. This represents the rate performances of 1, 2 and 3 wt. % of CeO<sub>2</sub> coated LiFePO<sub>4</sub> between 0.1 and 30 C rates under room temperature. The electrode discharge capacities are 151, 147, 126, 112, 65, 58 mAh/g for 1 wt. % of CeO<sub>2</sub>, 163, 160, 152, 147, 116, 75 mAh/g for 2 wt. % of CeO<sub>2</sub> and 157, 156, 141, 134, 111, 68 mAh/g for 3 wt. % of CeO<sub>2</sub> coated samples respectively, up to 10 cycles at 0.1, 0.5, 1, 10, 20 and 30 C rates. The aforementioned result of 2 wt. % CeO<sub>2</sub> coated LFP electrodes exhibits remarkable improvement in discharge capacity than the earlier reports viz., carbon, CeO<sub>2</sub> and other metal oxides coated LFP (Table 3).

Figure 7 (d-f) illustrate the 1, 2 and 3 wt. % of CeO<sub>2</sub> coated LFP samples for 100 cycles of discharge capacity with the coulombic efficiency at 1 C rate under room temperature. The coulombic efficiency of CeO<sub>2</sub> coated LFP composites are almost same (about 97-99 %) at 1 C rate for the coated samples. The 2 wt. % of CeO<sub>2</sub> coated LFP sample has shown an excellent rate with an appealing cyclic performance and more stable coulombic efficiency than the rest. It is observed that the coulombic efficiency has been improved upon increasing the CeO<sub>2</sub> content until 2 wt.%; further addition of CeO<sub>2</sub> affected this trend. This could be due to Ce<sup>4+</sup> is not electrochemically active and therefore, the presence of excess CeO<sub>2</sub> could lower the discharge capacity. [35] Consequently, the optimized amount of CeO<sub>2</sub> coating could improve the discharge capability and coulombic efficiency of the electrode materials.

The electrochemical kinetics of pristine and CeO<sub>2</sub> coated LiFePO<sub>4</sub> composite has been studied by Electrochemical

Impedance Spectroscopy (EIS). Figure 8 shows the Nyquist impedance plots of the materials and equivalent circuit (Inset of Figure 8). The Nyquist plots are composed of a semi-circle in the high frequency region and an inclined line in the low frequency region. The intercept of high frequency region corresponds to the ohmic resistance ( $R_e$ ), which represents the resistance of the electrolyte and electrode. The semicircle in the middle frequency range indicated the charge transfer resistance ( $R_{ct}$ ). The inclined line corresponds to the diffusion

of  $\text{Li}^+$  in the bulk electrode, namely the Warburg impedance ( $Z_w$ ). The charge-transfer resistance of  $\text{CeO}_2$  coated  $\text{LiFePO}_4$  electrodes are much less than that of pristine  $\text{LiFePO}_4$ . This indicates the coating is more favourable for the insertion and de-insertion of lithium ions during the charge and discharge process. Among the  $\text{CeO}_2$  coated  $\text{LiFePO}_4$  samples, the 2 wt. % of  $\text{CeO}_2$  coated  $\text{LiFePO}_4$  shows the smallest  $R_{ct}$  of  $230 \Omega$  and  $Z_w$ , which is clearly seen in the plots (Figure 8).

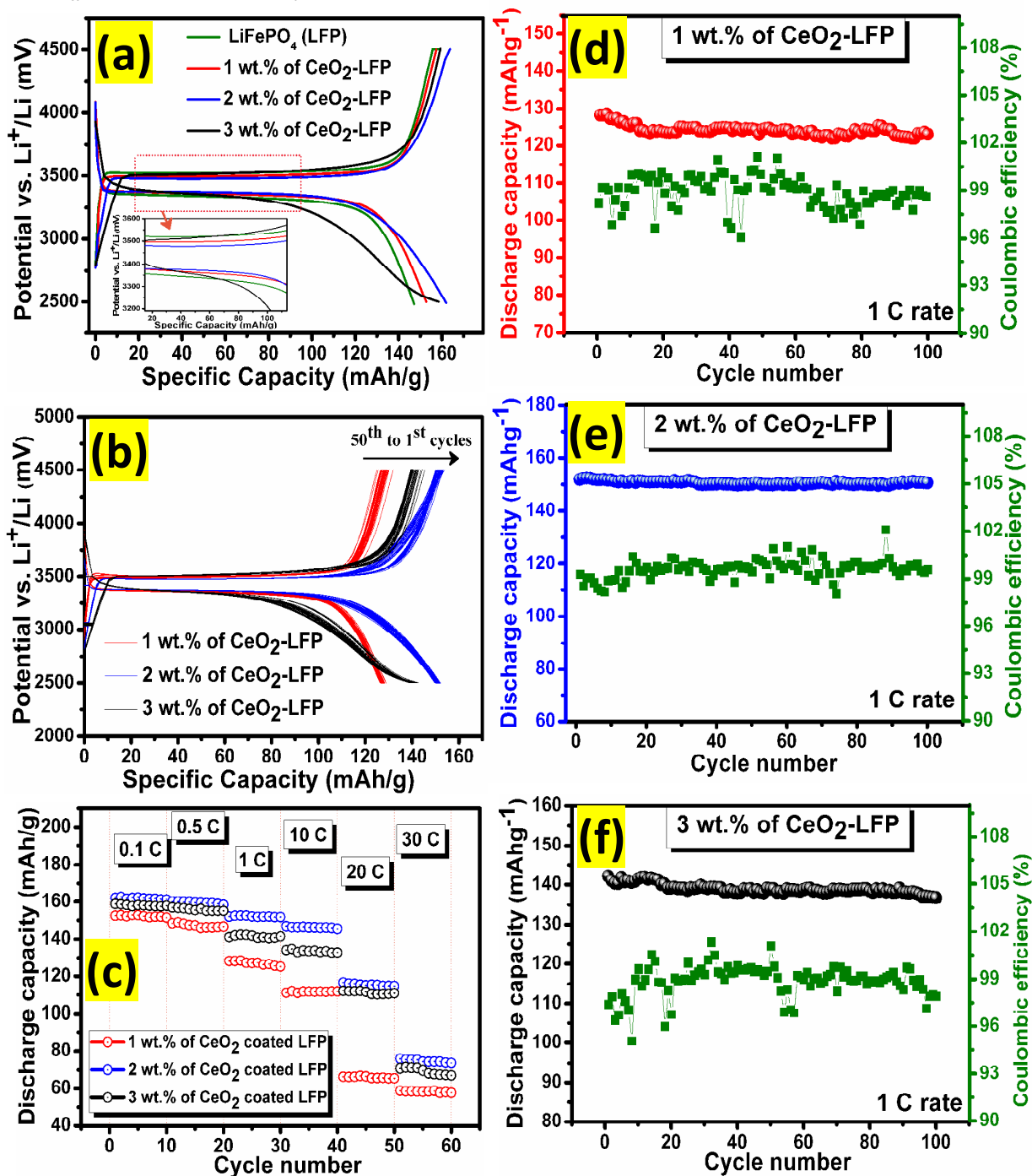
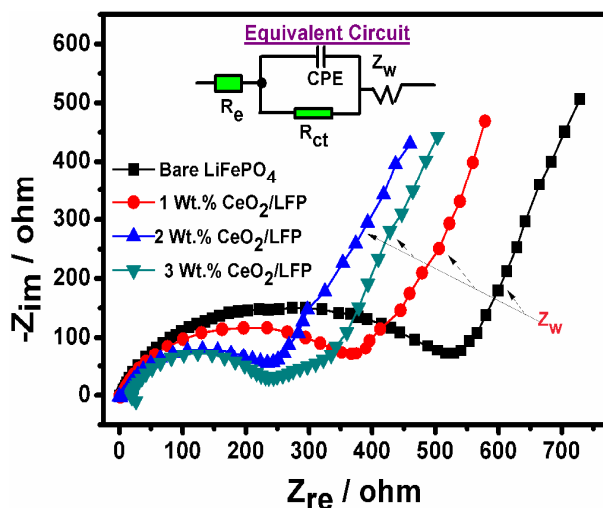


Fig. 7 Charge-discharge performance (a) bare and coated  $\text{LiFePO}_4$  at 0.1 C rate (b)  $\text{CeO}_2$  coated  $\text{LiFePO}_4$  at 1 C rate (c) rate performance of  $\text{CeO}_2$  coated  $\text{LiFePO}_4$  at various rates (d-f) Cyclic behaviour and coulombic efficiency of 1, 2 and 3 wt. % of  $\text{CeO}_2$  coated  $\text{LiFePO}_4$  at 1 C rate under room temperature, respectively.

**Table 3** The CeO<sub>2</sub> coated LiFePO<sub>4</sub> samples compared with earlier report of carbon, CNT, Graphene coated and Metal oxide modified LiFePO<sub>4</sub> samples.

Material name	Observed discharge capacity (mAh g <sup>-1</sup> ) with current rate of 0.1 C	Reference
LiFePO <sub>4</sub> and LiFePO <sub>4</sub> -CNT	129 and 155 at 10 mA/g	Wu et al.[40]
LiFePO <sub>4</sub> /C and Graphene/LiFePO <sub>4</sub> /C	146.5 and 157.8	Wang et al. [41]
C -LiFePO <sub>4</sub> and Graphene-LiFePO <sub>4</sub>	~150 and ~153	Kim et al.[42]
LiFePO <sub>4</sub> /Graphene	160.3	Wang et al.[43]
LiFePO <sub>4</sub> /rGO	161	Nagaraj et al.[44]
Sn-modified LiFePO <sub>4</sub> (Sn/Fe ratio of 1:99, 3:97 and 5:95)	122, 122 and 114	Ziolkowska et al. [13]
SiO <sub>2</sub> -coated LiFePO <sub>4</sub>	160	Li et al. [45]
LiFePO <sub>4</sub> /C/CePO <sub>4</sub>	156	Quan et al. [20]
2 wt.% of CeO <sub>2</sub> -coated LiFePO <sub>4</sub> /C	153.8	Yao et al. [16]
pristine LiFePO <sub>4</sub>	149	<b>In this work</b>
1wt. % of CeO <sub>2</sub> - LFP	153	
2 wt. % of CeO <sub>2</sub> - LFP	<b>163</b>	
3 wt. % of CeO <sub>2</sub> - LFP	159	

The small resistance indicates that Li<sup>+</sup> ion and electron transfer are more feasible on the electrode, which may be attributed to the decreasing electronic resistance of the composite material. The impedance plot of the bare and CeO<sub>2</sub> coated LFP electrodes are represented by a large depressed semicircle with inductive line and very small semicircle at room temperature, indicating a lower electronic/ionic conductivity of bare LFP than the values of CeO<sub>2</sub> coated LFP sample.



**Fig. 8** Nyquist plots of the bare and CeO<sub>2</sub> coated LiFePO<sub>4</sub> composite electrodes.

The impedance of the 2 wt. % of CeO<sub>2</sub> coated LiFePO<sub>4</sub> composite is significantly smaller than that of the other samples, which indicates an enhanced both ionic and electronic conductivity as well as lower interface impedance, relating to a superior rate performance. [37] CeO<sub>2</sub> can serve as

protective layer and prevents the direct contact between LiFePO<sub>4</sub> and the electrolyte solution like preformed SEI, which can reduce side reactions and improving the structure, cycle stability and decreasing charge-transfer resistance. [24] CeO<sub>2</sub> coating enhances the reversibility of electrode reaction. However, when the amount of CeO<sub>2</sub> is increased to 3 wt.%, the initial discharge capacity and cycling stability are descended, which may be due to excessive amount of CeO<sub>2</sub>. The 2 wt. % of CeO<sub>2</sub> coated on LiFePO<sub>4</sub> is found to be an optimum level of coating content which improves EC performance. [46]

#### 4. Conclusions

Olivine type orthorhombic structure of bare LiFePO<sub>4</sub> has been successfully prepared via polyol technique with Low boiling point solvent (DEG), simple binary precursor and also without post heat treatment, any special environment and carbon materials. In addition, the CeO<sub>2</sub> coated LFP has been subjected to one step short-time heat treatment without any change in bare LFP structure. Due to the heat treatment, particle size of coated samples has been reduced. The 2 wt. % of CeO<sub>2</sub> coated LFP surface was formed in thin layer. It exhibits the superior electrochemical performance than other coated and bare LFP samples. It denotes that the appropriate content of CeO<sub>2</sub> coating has better ionic and electronic conduction, which enhanced the ionic and electronic transport in the LiFePO<sub>4</sub> electrode. However, the higher content of inactive materials may be impeding the mass and charge transfer and reduce the reversible capacity. Therefore, an optimized content of CeO<sub>2</sub> protects the LiFePO<sub>4</sub> electrode from electrolyte corrosion and maintained the structural stability of the LiFePO<sub>4</sub>. It is beneficial to use in high-rate battery applications. This is due to the excellent rate capability and cycle stability of CeO<sub>2</sub> tailored LiFePO<sub>4</sub>.

## Acknowledgements

The authors M. Sivakumar and R. Muruganatham gratefully acknowledge for the financial support to carry out this work by Department of Science and Technology (DST), New Delhi, Govt. of India under DST-SERC major research project (SR/S2/CMP-0049/2008).

## Notes and references

- 1 A.K. Padhi, K.S. Nanjundaswamy, J.B. Goodenough, *J. Electrochem. Soc.* 1997, **144**, 1188-1194.
- 2 J. Wang, X. Sun, *Energy Environ. Sci.*, 2015, **8**, 1110-1138.
- 3 J-T. Son, *J. Korean Electrochem. Soc.* 2010, **13(4)**, 246-250.
- 4 F. Pan, W-l. Wang, *J Solid State Electrochem.* 2012, **16**, 1423-1427.
- 5 C-H. Hsu, H-Y. Liao, P-L. Kuo, *Energy Technol.* 2014, **2**, 409-413.
- 6 X. Rui, X. Zhao, Z. Lu, H. Tan, D. Sim, H. H. Hng, R. Yazami, T. M. Lim, Q. Yan, *ACS Nano* 2013, **7**, 5637-5646.
- 7 Y. Liu, C. Mi, C. Yuan, X. Zhang, *J. Electroanalytical Chem.* 2009, **628**, 73-80.
- 8 J. Wang, X. He, R. Kloepsch, S. Wang, B. Hoffmann, S. Jeong, Y. Yang, J. Li, *Energy Technol.* 2014, **2**, 188-193.
- 9 X. Zhi, G. Liang, L. Wang, X. Ou, L. Gao, X. Jie, *J. Alloy. Compd.*, 2010, **503**, 370-374.
- 10 B. Ding, G. Ji, Z. Sha, J. Wu, L. Lu, J. Y. Lee, *Energy Technol.* 2015, **3**, 63-69.
- 11 M. Sivakumar, R. Muruganatham, R. Subadevi, *Appl. Surf. Sci.* 2015, **337**, 234-240.
- 12 S. Liu, H. Wang, *Mater. Lett.* 2014, **122**, 151-154.
- 13 D. Ziolkowska, K.P. Korona, B. Hamankiewicz, S-H. Wu, M-S. Chen, J.B. Jasinski, M. Kaminska, A. Czerwinski, *Electrochim. Acta* 2013, **108**, 532-539.
- 14 M. Leblanc, V. Maisonneuve, A. Tressaud, *Chem. Rev.* 2015, **115**, 1191-1254.
- 15 G-M. Song, Y. Wu, Q. Xu, G. Liu, *J. Power Sources* 2010, **195**, 3913-3917.
- 16 J. Yao, F. Wu, X. Qiu, N. Li, Y. Su, *Electrochim. Acta* 2011, **56**, 5587-5592.
- 17 T-F. Yi, J-Z. Wu, M. Li, Y-R. Zhu, Y. Xie, R-S. Zhu, *RSC Adv.*, 2015, **5**, 37367-37376.
- 18 Q. Li, V. Thangadurai, *Fuel Cells* 2009, **09 (5)**, 684-698.
- 19 Y. Wang, C. X. Guo, J. Liu, T. Chen, H. Yang, C. M. Li, *Dalton Trans.*, 2011, **40**, 6388-6391.
- 20 W. Quan, Z. Tang, J. Zhang, Z. Zhang, *Mater. Chem. Phys.* 2014, **147**, 333-338.
- 21 D-H. Kim, J.K. Kim, *Electrochem. Solid-State Lett.* 2006, **9**, A439.
- 22 S. W. Oh, Z-D. Huang, B. Zhang, Y. Yu, Y-B. He, J-K. Kim, *J. Mater. Chem.* 2012, **22**, 17215.
- 23 F. Wu, *Electrochim. Acta* 2009, **54**, 6803-6807.
- 24 Y. Yang, R. Guo, G. Cai, C. Zhang, L. Liu, S. Wang, C. Wu, Y. Wan, *J. Electrochem. Soc.* 2014, **161 (14)**, A2153-A2159.
- 25 H-W. Ha, N. J. Yun, M. H. Kim, M. H. Woo, K. Kim, *Electrochim. Acta* 2006, **51**, 3297-3302.
- 26 W. Yuan, H.Z. Zhang, Q. Liu, G.R. Li, X.P. Gao, *Electrochim. Acta* 2014, **135**, 199-207.
- 27 S.J. Shi, J.P. Tu, Y.J. Zhang, Y.D. Zhang, X.Y. Zhao, X.L. Wang, C.D. Gu, *Electrochim. Acta* 2013, **108**, 441-448.
- 28 C.M. Burba, R. Frech, *J. Electrochem. Soc.* 2004, **151(7)**, A1032-A1038.
- 29 Y. Hou, X. Wang, Y. Zhu, C. Hu, Z. Chang, Y. Wu, R. Holze, *J. Mater. Chem. A*, 2013, **1**, 14713-14718.
- 30 B. Yan, H. Zhu, *J. Nanoparticle. Res.* 2008, **10**, 1279-1285.
- 31 W. Xiong, Q. Hu, S. Liu, *Anal. Methods*, 2014, **6**, 5708-5711.
- 32 A. Fedorková, R. Orináková, A. Orinák, M. Kupková, H.-D. Wiemhöfer, J.N. Audinot, J. Guillot, *Solid State Sciences* 2012, **14**, 1238-1243.
- 33 J. Ni, Y. Wang, *RSC Adv.*, 2015, **5**, 30537-30541.
- 34 S. A. Miller, V. Y. Young, C. R. Martin, *J. Am. Chem. Soc.*, 2001, **123**, 12335.
- 35 D. Arumugam, G.P. Kalaignan, *Electrochim. Acta* 2010, **55**, 8709-8716.
- 36 S. Gopukumar, C. Nithya, P. H. Maheshwari, R. Ravikumar, R. Thirunakaran, A. Sivashanmugam, S. K. Dhawanb, R. B. Mathur, *RSC Advances*, 2012, **2**, 11574-11577.
- 37 C. Wang, J. Hong, *Electrochemical and Solid-State Letters*, 2007, **10(3)**, A65-A69.
- 38 W. Wei, L. Guo, X. Qiu, P. Qu, M. Xu, L. Guo, *RSC Adv.*, 2015, **5**, 37830-37836.
- 39 H.-W. Ha, N. J. Yun, K. Kim, *Electrochim. Acta*, 2007, **52**, 3236.
- 40 G. Wu, Y. Zhou, X. Gao, Z. Shao, *Solid State Sciences*, 2013, **24**, 15-20.
- 41 Z. Wang, H. Guo, P. Yan, *Ceram. Int.* 2014, **40**, 15801-15806.
- 42 W.K. Kim, W.H. Ryu, D.W. Han, S.J. Lim, J.Y. Eom, H.S. Kwon, *ACS Appl. Mater. Interfaces* 2014, **6**, 4731-4736.
- 43 L. Wang, H. Wang, Z. Liu, C. Xiao, S. Dong, P. Han, Z. Zhang, X. Zhang, C. Bi, G. Cui, *Solid State Ionics* 2010, **181**, 1685-1689.
- 44 D. H. Nagaraju, M. Kuezman, G. S. Suresh, *J Mater Sci* 2015, **50**, 4244-4249.
- 45 Y-D. Li, S-X. Zhao, C-W. Nan, B-H. Li, *J. Alloy. Compd.*, 2011, **509**, 957-960.
- 46 J. Zhai, M. Zhao, D. Wang, and Y. Qiao, *J. Alloy. Compd.*, 2010, **502**, 401-406.

## Graphical Abstract

